The shear and extensional rheology of aqueous xanthan gum solution using the multi-mode Giesekus model.

Janaki Umashanker[1] and Bart Hallmark[1]

[1]University of Cambridge, Philippa Fawcett Drive, Cambridge CB3 0AS

ABSTRACT

Xanthan gum can often be used as a drilling fluid and as an experimental analogue for certain oil well drilling fluids as it is rheologically similar yet physically simpler. This paper presents rheology data in shear and extension for xanthan gum at 10 g/L concentration. These data are compared to predictions made with the multi-mode Giesekus constitutive equation using a unified set of parameters to model both the shear and extensional rheology.

Low shear rate rheology (0.05 to 500 s^{-1}) was acquired using an ARES rotational rheometer. The steady shear rheology is similar to that reported by Martín-Alfonso *et al*.[1]. A fully contained dual piston rheometer, the Multi Pass Rheometer (MPR), was used with a capillary die geometry to obtain the steady shear rheology at high shear rates (400 to 10,000 s^{-1}). The viscoelastic response of xanthan gum was measured using oscillatory tests on an ARES rheometer within the linear viscoelastic range. The extensional data for xanthan gum was obtained using a filament thinning rheometer: the Cambridge Trimaster (HB4). Flow visualisation tests were conducted on the MPR at high shear rates (400 to 10,000 s^{-1}) with a contraction-expansion geometry. A low concentration of sand particles was included to act as tracers to highlight the flow structure.

The Giesekus model[5] used with eight modes gave a reasonable fit to the entire set of steady shear, oscillatory shear, step strain stress relaxation and filament thinning data. These Giesekus parameters were then used to model the flow within the MPR's contraction-expansion geometry using OpenFOAM with the RheoTool plugin, developed by Pimenta and Alves[13]. This paper presents a comparison of the flow observed within the MPR and simulation data obtained at a maximum Weissenberg number of order 10^7.

INTRODUCTION

Drilling is a common operation that has historically been used to facilitate the extraction of oil and gas resources. Looking to the future, drilling has an important role to play in carbon capture and storage, since bores will need to be drilled into geologically suitable formations for carbon dioxide sequestration.

During the construction of a wellbore, a drill bit is used to drill into the rock beneath. A fluid, known as a drilling fluid, is circulated around the well to remove these cuttings to the surface, maintain formation pressure for stability and a selection of other functions. At the end of each section drilled, a large diameter steel pipe, known as casing, is cemented into the wellbore. To keep the drilling fluids and cement apart, spacer fluids are used during the displacement to prevent contamination.

These fluids, known as well construction fluids (WCFs), are subjected to a variety of processing conditions during operations. The

material response of these WCFs in both shear and extension is an essential component of their overall efficacy during the drilling process. A thorough understanding of the rheological behaviour of WCFs in both shear and extension is, therefore, required.

This paper explores the shear and extensional rheology of a biopolymer solution commonly encountered in WCFs, xanthan gum, at 10 g/L concentration. This concentration had been selected for the analysis due to the similar viscoelastic behaviour to a material used in well construction.

MATERIALS AND METHODS

Xanthan gum (Sigma Aldrich) is a hydrocolloid and is soluble in water. The concentration studied was 10 g/L, which is within the semi dilute regime. Aqueous solutions of xanthan gum in deionised water were prepared following the procedure highlighted by Martin-Alfonso and co-workers[1]. All rheometry tests were carried out at 20 °C.

RHEOMETERS

Shear rheometers

An ARES rheometer (Rheometric Scientific Inc.) was used to obtain steady shear and small angle oscillatory data. Xanthan gum was tested on the ARES rheometer using a cup and bob geometry. The dimensions of the geometry used on the ARES were: cup diameter 34 mm; bob diameter 32 mm and bob length 34 mm.

To obtain rheological data at high shear rates, a capillary rheometer was used. The Cambridge Multi Pass Rheometer (MPR, Strata Technology Ltd.) was used to investigate shear rates ranging between 400 s^{-1} and 100,000 s^{-1}. The geometries used for xanthan gum at 10 g/L were cylindrical capillaries of diameter 1 mm, and lengths 4 mm, 10 mm and 20 mm. Experiments using several different capillary dimensions were required to obtain data for the capillary rheometer correction factors[2].

Extensional rheometer

The Trimaster HB4 (Huxley Bertram Ltd.) was used to investigate the extensional rheology of both solutions. The HB4 is a capillary break-up device, which measures the diameter of a stretched fluid filament as it thins under the action of surface tension.

In use, a sample of fluid was placed in a 0.6 mm gap between two pistons, 1.2 mm in diameter. The pistons were then pulled apart at a velocity of 1 m/s until their separation distance was 1.6 mm. The filament of fluid that formed was filmed using a high-speed camera (Photron Fastcam 1024 PCI), operating at 18,000 frames per second with shutter speed 1.1×10^{-5} s. The camera resolution was 14.6 pixels per μm. Quantitative data for the change of filament diameter as a function of time was calculated as a post processing step by using the Trivision image analysis software.

Contraction tests on the MPR

Contraction flow consists of a combination of shear and extensional deformation. Observation of the resultant flow field is, hence, one way to examine how a material responds to the combined effect of these deformations. Using the MPR equipped with a slit die geometry, contraction flow was applied to 10 g/L xanthan gum seeded with a low concentration of sand particles having an average diameter of 0.2 mm. The setup for these tests follows that outlined by Hallmark and co-workers[3]: a planar geometry having a contraction ratio of 6.7:1 was used, and the resultant flow patterns were observed optically. The contraction flow tests were conducted in order of increasing piston speed, resulting in wall shear rates ranging between 400 s^{-1} and 100,000 s^{-1}

A series of additional experiments were performed to determine the influence of the sand particles on the xanthan gum rheology.

It was observed that sand particles augment the pressure drop when compared to xanthan gum alone, but the effects were small for low piston velocities: data has not been included here due to page constraints.

Optical observation of fluid flow is a simple and useful technique that allows experimental data to be compared with numerical flow prediction. A phenomenon that can occur in viscoelastic fluids is secondary flow in the form of vortices. Secondary flows are often formed due to the presence of elasticity and inertia and can cause pressure drops to both augment and become time-dependent at high shear rates. Secondary flow effects are well known and are widely described, for example in the work of Baloch *et al*.[4].

RHEOLOGICAL MODELS

Many different viscoelastic models exist, which can be used to describe both linear and non-linear behaviour in steady shear. The shear thinning nature of xanthan gum requires use of a non-linear viscoelastic model, of which the Giesekus model[5] is one of the simplest. A distinct advantage of the Giesekus model is that it can be solved analytically for various simple deformations. The resultant analytical expressions can be fitted to experimental data, thus allowing Giesekus parameters to be calculated for a given material with relative ease.

In this paper, the multi-mode Giesekus model was used to fit experimental data resulting from steady shear, small angle oscillatory, stress relaxation and filament thinning tests. To obtain the single set of uniform parameters, a MATLAB® script was written that fitted Eqs. 2, 5, 6, 7 and 9 to rheological data. This script solved a minimisation problem where the objective function was a logarithmic form of the coefficient of determination. Logarithmic form was used due to the wide range of numerical values of equal significance that required fitting.

The Giesekus constitutive model

The Giesekus model is used to describe the dynamics of packed polymer chains dispersed in a Newtonian solvent. The behaviour of some fluids, especially those with a range of molecular weights, cannot be captured accurately with a single relaxation time, hence multi-mode models can be used to capture the effects due to a range of relaxation timescales. A general statement of the multi-mode Giesekus model, having i relaxation modes such that $\boldsymbol{\tau} = \sum_i \boldsymbol{\tau}_i$ and where the stress contribution from the solvent can be neglected, is shown in Eq. 1.

$$\frac{\boldsymbol{\tau}_i}{\lambda_i} + \frac{\partial \boldsymbol{\tau}_i}{\partial t} + \mathbf{v}\nabla\boldsymbol{\tau}_i - \left((\nabla\mathbf{v})^{\mathrm{T}}\boldsymbol{\tau}_i + \boldsymbol{\tau}_i(\nabla\mathbf{v})\right) = -\frac{\eta_{0,i}}{\lambda_i}\dot{\boldsymbol{\gamma}} + \frac{a_i}{\eta_{0,i}}\boldsymbol{\tau}_i \cdot \boldsymbol{\tau}_i \quad (1)$$

Here:

$\eta_{0,i}$ = i^{th} zero shear rate viscosity (Pa.s)
a_i = Mobility factor for mode i
λ_i = Relaxation time for mode i (s)
$\boldsymbol{\tau}_i$ = Stress tensor for mode i (Pa)
$\boldsymbol{\tau}$ = Stress tensor (Pa)
$\mathbf{v}$ = Velocity vector (m.s^{-1})
t = Time (s)
$\dot{\boldsymbol{\gamma}}$ = $\nabla\mathbf{v} + \nabla\mathbf{v}^{\mathrm{T}}$ – shear rate tensor (s^{-1})

Solutions to Eq. 1 are presented in the literature for different flow fields. Two flow fields relevant to this study are steady shear, and uniaxial extension.

Expressions for steady shear

In steady shear, $\dot{\boldsymbol{\gamma}} = \dot{\gamma}_{xy}\begin{bmatrix}0 & 1 & 0\\ 1 & 0 & 0\\ 0 & 0 & 0\end{bmatrix}$. It can be shown that the steady shear viscosity, η_S, predicted by Eq. 1, can be written as Eq. 2[6].

$$\eta_S = \sum_i \eta_{0,i}\frac{\left(1-f_{i,G}\right)^2}{1+(1-2a_i)f_{i,G}} \quad (2)$$

Here:

$$f_{i,G} = \frac{1-X_{i,G}}{1+(1-2a_i)X_{i,G}} \quad (3)$$

$$X_{i,G}^2 = \frac{-1+\sqrt{1+16a_i(1-a_i)(\lambda\dot{\gamma})^2}}{8a_i(1-a_i)(\lambda\dot{\gamma})^2} \quad (4)$$

Expressions for small angle oscillatory shear

For small displacement gradients (SDGs), such as small angle oscillatory shear, the quadratic stress term in Eq. 1 can be neglected. Also, for SDGs, simple differential form can be used in place of upper convected form. These simplifications allow the elastic and viscous modulii for multi-mode Giesekus to be written in Maxwellian form as shown in Eqs. 5 and 6.

$$G_G^{'}(\omega) = \sum_{i=1}^{N} \frac{g_i\lambda_i^2\omega^2}{(1+\omega^2\lambda_i^2)} \quad (5)$$

$$G_G^{''}(\omega) = \sum_{i=1}^{N} \frac{g_i\lambda_i\omega}{(1+\omega^2\lambda_i^2)} \quad (6)$$

Here:
G'_G = Elastic modulus (Pa)
G_G'' = Viscous modulus (Pa)
g_i = Material modulus (Pa)

Expressions for stress relaxation

When examining stress relaxation behaviour after the application of a step strain, γ, the relaxation modulus must be calculated as a function time, $G_R(t,\gamma)$. An expression for $G_R(t,\gamma)$ for the multi-mode Giesekus model has been derived by Holz *et al.*[6] and is shown in Eq. 7.

$$G_R(t,\gamma) = \sum_i \frac{\tau_{xy,i}}{\gamma_i}$$
$$= \sum_i \frac{g_i}{\exp\left(\frac{t}{\gamma_i}\right)+2a_i^2\gamma^2\left(1-\cosh\left(\frac{t}{\gamma_i}\right)\right)+a_i\gamma^2\left(\exp\left(\frac{t}{\gamma_i}\right)-1\right)} \quad (7)$$

Here:
$\tau_{xy,i}$ = x,y element of $\boldsymbol{\tau}$ for mode i (Pa)

Expressions for extensional filament thinning

In uniaxial extension, $\dot{\boldsymbol{\gamma}} = \dot{\gamma}_{zz}\begin{bmatrix} -\frac{1}{2} & 0 & 0 \\ 0 & -\frac{1}{2} & 0 \\ 0 & 0 & 1 \end{bmatrix}$.

Solutions to the Giesekus constitutive equation have been derived that predict the normalised diameter, D/D_0, of a fluid filament thinning as a function of time, t, under the action of surface tension, α, alone for both single-[7] and multi-mode[8] forms. The normalisation parameter is the initial filament diameter, D_0.

Extending the filament thinning analysis to multiple relaxation modes is non-trivial, and results in an ordinary differential equation (ODE) that requires numerical solution. A key assumption in solving this ODE is that the axial stress, τ_{zz}, is initially distributed in inverse proportion to the magnitude of the N relaxation times[9] *viz*

$$\tau_{zz,i} = \frac{\lambda_{N-i+1}}{\sum_{i=1}^{N}\lambda_i} \times \frac{2\alpha}{D} \quad (8)$$

The result for multi-mode form can be written as shown below.

$$\frac{dD}{dt} = \frac{-\sum_i \frac{a_i}{\eta_0}\tau_{zz,i}^2 - \sum_i \frac{\tau_{zz,i}}{\lambda_i}}{\left(\frac{6\alpha}{D^2}+\frac{4}{D}\sum_i \frac{\eta_{0,i}}{\lambda_i}\right)} \quad (9)$$

RESULTS AND DISCUSSION

Steady shear flow

Flow curves showing the apparent shear viscosity as a function of shear rate for xanthan gum at concentration of 10 g/L, obtained from rotational and capillary rheometry, are shown in Fig. 1. Included in this plot is the prediction of Eq. 2 using 8 modes: parameters for these 8 modes are given in Table 1. Standard deviation error bars have been included with the capillary rheometry data.

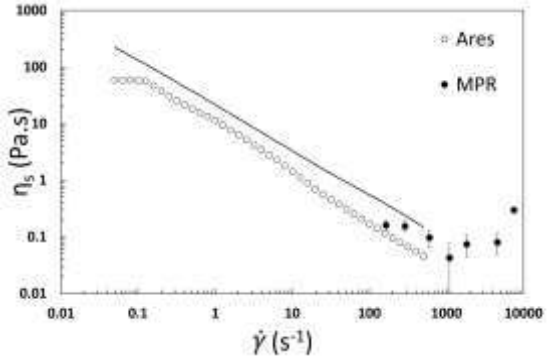

Figure 1: Apparent viscosity as a function of shear rate for xanthan gum at 10 g/L concentration. Data obtained from rotational (open points) and capillary (closed points) rheometry compared to Eq. 2 (solid line).

Table 1: Giesekus model parameters for 8 modes.

Mode	Giesekus parameters		
	a_i (-)	λ_i(s)	g_i (Pa)
1	0.000309	0.00100	2.02
2	0.110	0.0153	21.2
3	0.210	0.428	1.68
4	0.454	0.207	8.85
5	0.499	21.7	8.40
6	0.499	2.13	7.14
7	0.196	18500	0.609
8	0.410	1730	3.00

MPR data for xanthan gum was corrected using the Rabinowitsch and Bagley corrections[3]. The maximum Reynolds number within the MPR was 0.22, indicating creeping, non-inertial, flow.

It can be seen from Fig. 1 that xanthan gum at 10 g/L concentration is prone to shear thinning over the range of shear rates investigated. Shear thinning occurs in polymer solutions when the polymer chains start to disentangle, causing the viscosity of fluid to decrease with increasing shear rate.

Prior to shear thinning, xanthan gum displays a plateau viscosity at shear rates below about 0.1 s^{-1}. This behaviour matches existing literature data for the same concentration[1].

The discontinuity between rotational and capillary data for xanthan gum is likely due to the presence of vortices at the entrance of the capillary. Li and co-workers[10] demonstrate that vortices upstream of a contraction augment the pressure drop measured across the contraction. Apparent viscosity data yielded by capillary rheometry are derived from pressure drop measurements, hence the presence of vortices likely explain this viscosity mismatch.

The Giesekus model fitted with the steady shear data from the ARES has shown a decreasing viscosity with increasing shear rate. However, the fitted model shows significant quantitative difference between the experimental data set, having a low coefficient of determination, $R^2 = 0.44$. This is due to using a unified set of parameters for the Giesekus model that attempts to describe all deformation behaviour: this fit is, therefore, a compromise.

Small angle oscillatory shear

The variation of elastic and viscous moduli as a function of frequency for xanthan gum with concentration 10 g/L is shown in Fig. 2. The frequency sweep used a strain that was within the linear viscoelastic range. Using a strain sweep test, the results of which are not shown in this paper due to page constraints, the chosen strain was 10%.

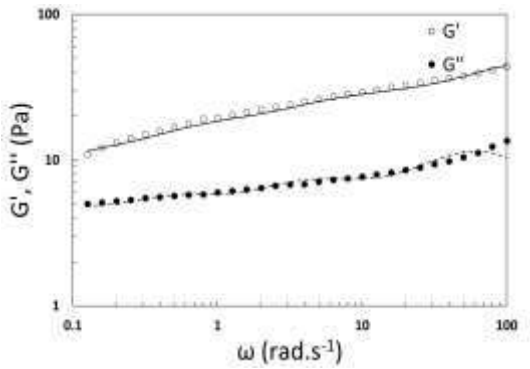

Figure 2: Variation of G' (open points) and G'' (closed points) as a function of angular frequency for xanthan gum shown with the prediction of Eq. 5 (solid line) and Eq. 6 (dashed line).

Fig. 2 clearly shows that $G' > G''$ over the range of angular frequencies tested, demonstrating that xanthan gum is a strongly viscoelastic fluid. The xanthan gum behaviour is, again, consistent with that given in the literature[1,7]. Eq. 5 and Eq. 6 fit

the experimental data well, with coefficients of determination of $R^2 = 0.98$ and $R^2 = 0.88$, respectively.

Stress relaxation after step strain

Fig. 3 presents the stress relaxation modulus as a function of time for 10%, 100% and 200% strain. Plotted alongside these data are the predictions of Eq. 7.

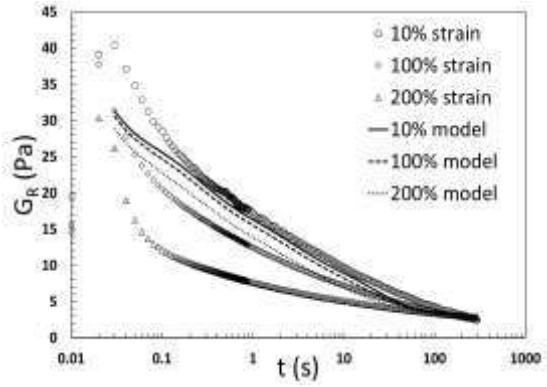

Figure 3: Step strain curves for xanthan gum at 10 g/L (open data points) compared with the predictions of Eq. 7 (lines).

The results in Fig. 3 show a general decrease of the relaxation modulus as a function time. This behaviour suggests that a lightly cross-linked network is present in the sample of xanthan gum at 10 g/L, consistent with the sharp decrease in the relaxation modulus as highlighted by Fujii and colleagues[11]. The trends shown in Fig. 3 also show that as the strain increases, the rate of change of the relaxation modulus also increases with time. This shows that faster relaxation is obtained when higher strains are applied, as highlighted in literature by Nam and co-workers[12].

The predictions of Eq. 7 using the parameters given in Table 1 are also shown in Fig. 3. Whilst stress decay behaviour is captured in a broadly qualitative manner, a quantitative match is not obtained. It can be deduced that this is due to using a unified set of parameters, which results in some data sets having a stronger quantitative match compared to others. Coefficients of determination for 10%, 100% and 200% strain are $R^2 = 0.96$, $R^2 = 0.86$ and $R^2 = 0.19$ respectively.

Filament thinning behaviour

In Fig. 4, the images of the fluid filament during deformation show a cylindrical filament with a smooth surface that thins uniaxially over time. The rate of filament thinning is influenced by surface tension, inertia, along with elastic and viscous forces. For tests conducted on the HB4, the Reynolds number was 0.026, indicating that inertial forces are negligible. A surface tension value of $\alpha = 0.0606$ N/m and an initial filament diameter of $D_0 = 2.73 \times 10^{-7}$ m was used in Eq. 8 and Eq. 9 to obtain the loci of points shown in Fig. 4. The surface tension value was obtained using the sessile drop method. The value quoted in this paper is the mean of five experimental results, with the data taking a range of ±0.001 N/m.

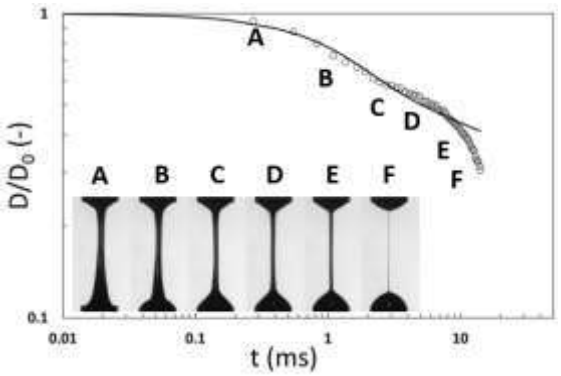

Figure 4: Normalised filament diameter as function of time for xanthan gum at 10 g/L (open points), shown with corresponding filament images. Prediction of Eq. 9 shown as a solid line.

Fig. 4 shows a general decrease in diameter of the filament over time with inflection points at 0.1 ms and 1 ms. Previous work[7] has shown that inflection points in filament thinning data can be described by multiple relaxation times. This further justifies the use of a multi-mode constitutive

model such as Giesekus. The coefficient of determination between the prediction of Eq. 9 using the parameters in Table 1 and the experimental data is $R^2 = 0.89$.

Observations and comments

A unified set of Giesekus parameters has been used with varying success to capture the shear and extensional behaviour of xanthan gum at 10 g/L concentration. It can be observed that the quantitative match between theory and experiment is better for smaller deformations than it is for larger deformations. This suggests that either a greater number of relaxation modes are required to better capture the non-linear behaviour, or that the Giesekus model is only capable of capturing a subset of the material response. More complex viscoelastic models exist, but they are not typically amenable to analytical solution. This, in turn, makes the parameter fitting procedure described in this paper significantly more challenging.

Contraction flow: experimental observation and numerical prediction

Initial results from contraction flow tests are reported here alongside initial data from numerical modelling carried out using OpenFOAM with the RheoTool plugin by Pimenta and Alves[13]. The MPR flow geometry and conditions, along with the rheological parameters given in Table 1, were used as input parameters for OpenFOAM simulations.

Fig. 5 compares the observed and predicted flow-fields. The stagnation zone observed experimentally upstream of the contraction is consistent with the presence of a slow-moving vortex, which is captured in the simulation. The plot in Fig. 6 compares the measured and predicted values of pressure drop.

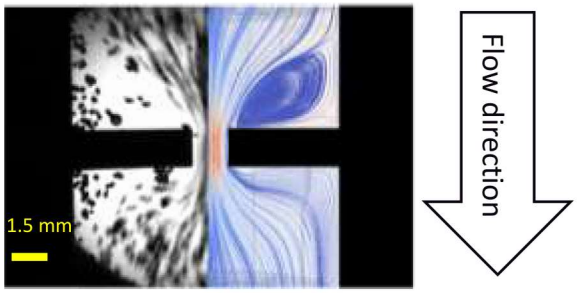

Figure 5: Comparison of streamlines rom experiment (A) and simulation (B) for xanthan gum 10 g/L at 10 mm.s^{-1} piston speed.

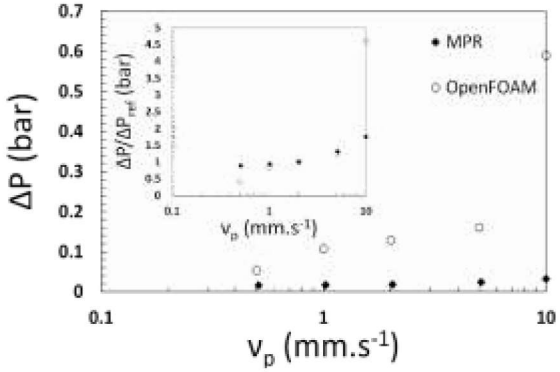

Figure 6: Comparison of MPR (closed points) and OpenFOAM (open points) pressure drop measurements over a range of piston velocities. Inset is a comparison of normalised pressure drop using a reference pressure drop measured at 2 mm.s^{-1}.

Examining Fig. 6, the numerically predicted pressure drop significantly exceeds the experimentally measured data. However, it was shown in Fig. 1 that Eq. 2 significantly over-predicted the shear viscosity when using the parameters in Table 1. If this over-prediction was the cause of the discrepancy, then plotting normalised pressure data should result in self-similar trends.

The normalised pressure data shown in the inset to Fig. 6 demonstrates that whilst the pressure drops for $1 \leq v_p \leq 5$ mm.s^{-1} are self-similar, significant deviation is present outside of this range. Elevated pressure drops can be caused by secondary flow, hence it is suggested that numerical simulation under-predicts the extent of secondary flow at low

piston speed and over-predicts the effect at high piston speed.

CONCLUSIONS

Rheological data for xanthan gum at a concentration of 10 g/L has been successfully obtained in both shear and extension. These data have been fitted to the multi-mode Giesekus model using a single set of unified parameters to describe all deformation behaviour. The experimental data was predicted semi-quantitatively for small deformations, notably the elastic and viscous moduli, and small strain relaxation behaviour. The qualitative experimental trends were captured by multi-mode Giesekus for larger deformations when the nonlinear viscoelastic response became significant. A quantitative match was not possible for these large deformations.

Numerical simulations carried out using OpenFOAM showed a good qualitative prediction of the experimentally observed flow field. The quantitative data suggests that the intensity of secondary flows is not accurately captured by numerical simulation for all experimental conditions.

REFERENCES

[1]Martín-Alfonso J.E., A.A. Cuadri M. Berta, and M. Stading. 2018. "Relation between Concentration and Shear-Extensional Rheology Properties of Xanthan and Guar Gum Solutions." Carbohydrate Polymers 181 (February): 63–70.

[2]Mackley M. R., Marshall R. T. J., and Smeulders J. B. A. F. "The Multipass Rheometer." *Journal of Rheology* 39, no. 6 (1995): 1293–1309.

[3]Hallmark B., Chen C.-H., and Davidson J.F. "Experimental and simulation studies of the shape and motion of an air bubble contained in a highly viscous liquid flowing through an orifice constriction." *Chemical Engineering Science*, 206 (2019): 272–288.

[4]Baloch A., P. Townsend and M.F. Webster. 1996. "On Vortex Development in Viscoelastic Expansion and Contraction Flows." Journal of Non-Newtonian Fluid Mechanics 65 (2-3): 133–49.

[5]Giesekus H. "A Simple Constitutive Equation for Polymer Fluids Based on the Concept of Deformation-Dependent Tensorial Mobility." *Journal of Non-Newtonian Fluid Mechanics*, 11 (1982): 69-109.

[6]Holz, T., Fischer, P. and Rehage, H. "Shear relaxation in the nonlinear-viscoelastic regime of a Giesekus fluid." *Journal of Non-Newtonian Fluid Mechanics*, 88 no. 1-2 (1999): 133–148.

[7]Armstrong R. C., Hassager O., and Bird R.B. *Dynamics of Polymer Liquids*. New York: Wiley, 1977.

[8]Torres M. D., Hallmark B., Wilson D.I., and Hilliou L. "Natural Giesekus Fluids: Shear and Extensional Behavior of Food Gum Solutions in the Semidilute Regime." *AIChE Journal* 60, no. 11 (2014): 3902–15.

[9]Hallmark B., D. Wilson D.I., and Pistre N. "Characterization of Extensional Rheological Filament Stretching with a Dual-Mode Giesekus Model." *AIChE Journal* 62, no. 6 (2016): 2188–99.

[10]Li Z., Yuan X.-F., Haward S.J., Odell J.A. and Yeates S., "Non-linear dynamics of semi-deilute polydisperse polymer solutions in microfluidics: effects of flow geometry". *Rheologica Acta*, 50 (2011): 277-290.

[11]Fujii S., Sasaki Y. and Orihara H. "Nonlinear Rheology and Fracture of Disclination Network in Cholesteric Blue Phase III". *Fluids*, 3, no. 2 (2018): 34.

[12]Nam S., Hu H. K., Butte J M., Chaudhuri O. "Strain-enhanced stress relaxation impacts nonlinear elasticity in collagen gels" *Proceedings of National*

Academy of Sciences, 113, no. 20 (2016): 5492-5497.

[13]Pimenta, F. and Alves, M.A. "Stabilization of an open-source finite-volume solver for viscoelastic fluid flows" *JNNFM*, 239 (2017): 85–104.